

## Observation of Tensor and Scalar Mesons Produced in $e^+e^-$ Annihilation at 29 GeV

S. Abachi, P. Baringer, B. G. Bylsma, R. DeBonte, D. Koltick, F. J. Loeffler, E. H. Low,  
R. L. McIlwain, D. H. Miller, C. R. Ng, L. K. Rangan,<sup>(a)</sup> and E. I. Shibata  
*Purdue University, West Lafayette, Indiana 47907*

M. Derrick, K. K. Gan,<sup>(b)</sup> P. Kooijman, J. S. Loos,<sup>(c)</sup> B. Musgrave, L. E. Price, J. Repond,  
K. Sugano, J. M. Weiss,<sup>(d)</sup> and D. E. Wood<sup>(a)</sup>  
*Argonne National Laboratory, Argonne, Illinois 60439*

D. Blockus, B. Brabson, J.-M. Brom, C. Jung, H. Ogren, and D. R. Rust  
*Indiana University, Bloomington, Indiana 47405*

C. Akerlof, J. Chapman, D. Errede, P. Kesten,<sup>(e)</sup> D. I. Meyer, D. Nitz, A. A. Seidl,<sup>(a)</sup> R. Thun, and  
M. Willutzky<sup>(f)</sup>  
*University of Michigan, Ann Arbor, Michigan 48109*

and

B. Cork  
*Lawrence Berkeley Laboratory, Berkeley, California 94720*  
(Received 23 June 1986)

The production of the tensor mesons  $f^0(1270)$  and  $K^{*0}(1430)$  and the scalar meson  $S(975)$  has been observed in  $e^+e^-$  annihilation at 29 GeV center-of-mass energy by use of data obtained with the high-resolution spectrometer at the SLAC  $e^+e^-$  storage ring PEP. The mean multiplicities for meson momenta greater than 1450 MeV/c are  $\langle n_{f^0} \rangle = 0.11 \pm 0.04$ ,  $\langle n_{K^{*0}(1430)} \rangle = 0.10 \pm 0.06$ , and  $\langle n_S \rangle = 0.05 \pm 0.02$  per hadronic event. The fragmentation functions of the tensor mesons are in good agreement with the predictions of the Webber cluster model. The data are consistent with a predominant strange-quark content of the  $S$  meson.

PACS numbers: 13.65.+i

The study of meson production in high-energy  $e^+e^-$  annihilation is important for understanding quark fragmentation and the detailed mechanisms that lead to the meson states. The production of vector and pseudoscalar mesons in high-energy  $e^+e^-$  annihilation has been reported.<sup>1,2</sup> From spin and statistics, the number of directly produced vector mesons is expected to be 3 times that of their pseudoscalar partners. This expectation is not supported by the data and thus vector-meson production must be modified by other effects. In the Lund string model,<sup>3</sup> the suppression of the vector mesons has been explained in part by the quark spin-spin interaction.<sup>4</sup> In the Webber cluster model<sup>5</sup> the higher masses of the vector mesons lead to a phase-space suppression. The question of whether similar effects occur in the production of  $J^{PC} = 2^{++}$  states has not been answered because of the lack of data.<sup>6</sup> In this paper we report the first measurements in  $e^+e^-$  annihilation at  $\sqrt{s} = 29$  GeV of the production of the tensor mesons  $f^0(1270)$  and  $K^{*0}(1430)$  from their decay channels  $\pi^+\pi^-$  and  $K^\pm\pi^\mp$ , respectively.

We also observe the production of the scalar meson  $S(975)$  through its  $\pi^+\pi^-$  decay channel. In the conventional  $q\bar{q}$  model of mesons, the  $S$  is a  $P$ -wave  $0^{++}$  state. However, it has been suggested that it may be-

long to a low-lying  $q\bar{q}q\bar{q}$  nonet,<sup>7</sup> or that it may be a purely gluonic state.<sup>8</sup> The possibility that the  $S$  meson may be a four-quark  $K\bar{K}$  bound state has also been proposed.<sup>9</sup> The measurements of the scalar-meson production in  $e^+e^-$  annihilation may help clarify the above speculations.

For this analysis we have used a data sample corresponding to an integrated luminosity of  $300 \text{ pb}^{-1}$  collected at the high-resolution spectrometer at the SLAC  $e^+e^-$  storage ring PEP. These data correspond to about  $120 \times 10^3$  hadronic events. The high-resolution spectrometer detector consists of seventeen cylindrical drift layers surrounded by a lead-scintillator shower counter, all contained in a 16.2-kG solenoidal magnetic field. A detailed description of the detector and the selection procedures for the hadronic events have been reported elsewhere.<sup>1,10</sup>

To ensure a clean sample of hadronic events, several criteria were imposed on the events and tracks. Only those events for which the average momentum per charged track was greater than 0.2 GeV/c were accepted. Events with fewer than five tracks were rejected. In all remaining events, tracks were rejected if they failed to register in more than 50% of the drift-chamber layers available to them, or if they formed an angle with respect to the beam direction of less than

26° or greater than 154°. Finally, it was required that the tracks originate from the interaction point and that their momentum transverse to the beam exceed 0.125 GeV/c.

Since no particle identification was used, all tracks passing the above cuts were considered as pion and kaon candidates and were used to calculate the  $\pi^+\pi^-$  and  $K^\pm\pi^\mp$  invariant masses. The doubly charged  $\pi^\pm\pi^\pm$  and  $K^\pm\pi^\pm$  spectra were also generated. A reduction in the combinatorial background of the mass spectra was obtained by requiring that  $|\cos\theta^*| < 0.65$ , where  $\theta^*$  is the decay angle in the rest frame of the two-particle system. This cut reduces the high combinatorial background observed for the two-particle systems with one particle produced backward in the rest frame. After the imposing of the above cuts, the mass spectra obtained for doubly charged combinations were parametrized by an empirical function<sup>11</sup> and were subsequently subtracted from the corresponding neutral-charge combinations.<sup>12</sup>

Figure 1(a) shows the measured  $\pi^+\pi^-$  mass spectrum between 0.64 and 1.62 GeV after subtraction of the parametrized like-charge combinations. These data were selected with  $x > 0.2$ , where  $x$  is the fractional momentum of the two-particle system ( $x = p/p_{\text{beam}}$ ). Figure 1(b) shows the equivalent spectrum for the  $K\pi$  combinations with mass between 0.8 and 1.67 GeV and with  $x > 0.2$ . The production characteristics of the  $f^0$ ,  $K^{*0}(1430)$ , and  $S$  mesons were extracted from these spectra by an overall fitting procedure. The lack of particle identification means that the mass spectra contain significant contributions from reflections due to misassignments. The mass spectrum of Fig. 1(a) was fitted by our assuming contributions from the  $\rho$ ,  $S$ , and  $f^0$  signals, as well as reflections from  $K^{*0}(892)$  and  $K^{*0}(1430)$ . The fit also includes a residual background term with the same functional form as that used to fit the doubly charged mass spectra. This additional term is required because of the reflections of various wide resonances and other systematic differences (such as long-range charge correlations) between the neutral and doubly charged mass spectra. The mass spectrum of Fig. 1(b) was fitted with contributions from the  $K^*(892)$  and  $K^*(1430)$  signals and their reflections,<sup>13</sup> and from the  $\omega$ ,<sup>14</sup>  $\rho$ ,  $S$ , and  $f^0$  reflections as well as a residual background.

Relativistic Breit-Wigner shapes with momentum-dependent widths were used for the resonances. Reflected spectra were reconstructed from pure resonance samples generated with the Lund Monte Carlo program<sup>15</sup> and processed through the full detector simulator, with inclusion of all analysis cuts. These were then parametrized by an empirical function.<sup>16</sup> The normalization factor of the parametrized  $K^*(892)$  ( $\rho$ ) reflection relative to that of the  $\rho$  [ $K^*(892)$ ] signal in the  $\pi\pi$  ( $K\pi$ ) mass spectrum was fixed to the

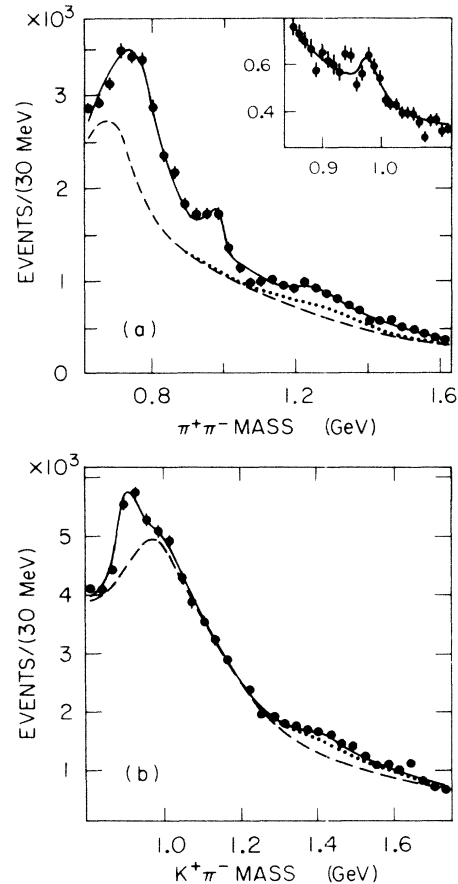


FIG. 1. (a)  $\pi^+\pi^-$  mass spectrum after subtraction of the doubly charged  $\pi^\pm\pi^\pm$  combinations. The solid curve is the overall fit which includes resonances, reflections, and phase-space background discussed in the text. Reflections and background contributions are shown by the dashed and dotted curves. Inset:  $S$ -meson mass region with a smaller bin size of 10 MeV. (b) Similar plot for the  $K^\pm\pi^\mp$  mass spectrum after subtraction of the doubly charged  $K^\pm\pi^\pm$  combinations.

value determined from our Lund Monte Carlo-generated events. The parameters of the Lund Monte Carlo simulation have been set to reproduce our previous measurements of vector mesons.<sup>1</sup> The effect of the reflection of  $S$  into the  $K\pi$  spectrum was determined from the  $S$  signal in the  $\pi\pi$  mass spectrum.

A different technique was used to fix the normalization factors of the  $K^*(1430)$  and  $f^0$  reflections. These normalizations are important since the reflection of  $K^*(1430)$  in the  $\pi\pi$  combination falls directly at the  $f^0$  mass, and vice versa. Since the relative yields of  $K^*(1430)$  and  $f^0$  have not been previously measured, an iterative procedure was used. As a starting point, the  $\pi\pi$  and  $K\pi$  mass spectra were simultaneously fitted by the assumption that the yields of  $f^0$  and  $K^*(1430)$  mesons were the same. The resulting relative yields of the  $f^0$  and  $K^*(1430)$  mesons were then

used in a new fit. This process was repeated until changes in the number of  $f^0$  and  $K^*(1430)$  events between two consecutive iterations were small. The convergence of this iterative procedure is possible because of the significant differences in the widths of the  $K^*(1430)$  ( $\sim 100$  MeV) and the reflection of  $f^0$  ( $\sim 300$  MeV). It should also be noted that the final tensor-meson rates were not sensitive to the starting values of the fitting procedure.

The solid curves in Figs. 1(a) and 1(b) which show the final fits have  $\chi^2/\text{d.o.f.}$  of 32/29 and 35/28, respectively. An increase of 20 (9) in the  $\chi^2$  resulted when the fit on the  $\pi\pi$  ( $K\pi$ ) spectrum was repeated without the  $f^0$  [ $K^*(1430)$ ] resonance term. In the  $\pi\pi$  spectrum the  $\chi^2$  was increased by 14 when the  $S$  meson was ignored in the fit.

In Fig. 1(a) clear contributions can be seen from the  $\rho$ ,  $f^0$ , and  $S$  mesons. In the fits, the masses and widths of the resonances were fixed to their established values.<sup>17</sup> For the narrow  $S$  signal, the detector mass resolution of 15 MeV was added to the width in quadrature. The dashed curve in this figure shows the contributions from the smooth background and the reflection from the  $K^*(892)$  events. The area between the dotted and dashed curves represents the reflection of the  $K^*(1430)$  peak.

In Fig. 1(b) the contributions from  $K^*(892)$  and  $K^*(1430)$ , whose masses and widths were again fixed to the known values, are evident. The dashed curve in this figure shows the contributions from phase-space background and all the reflections except that of the  $f^0$ , which is indicated in the figure by the dotted curve.

To estimate the mass and the width of the narrow  $S$  signal, we allowed these parameters to vary. The above fitting procedure was repeated on the  $\pi\pi$  mass spectrum with a narrower mass binning of 10 MeV. The solid curve in the inset of Fig. 1(a) shows the result of this fit in the  $S$ -signal region. After correcting for the detector resolution, we find a mass of  $978 \pm 9$  MeV and a full width of  $29 \pm 13$  MeV for the  $S$  peak. These values are in agreement with the world-average values of 975 and 33 MeV.<sup>17</sup> To estimate the masses and widths of the  $f^0$  and  $K^*(1430)$ , we used the  $\pi\pi$  and  $K\pi$  mass spectra obtained for  $0.4$

$< x < 0.7$ . This selection gave the most prominent signals for the above resonances. By repeating the overall fits and allowing the masses and widths of the tensor mesons to vary, we measure mass values of  $1288 \pm 12$  MeV and  $1432 \pm 34$  MeV, and full widths of  $170 \pm 52$  MeV and  $86 \pm 67$  MeV for the  $f^0$  and  $K^*(1430)$  signals, respectively.

Differential cross sections were measured by our repeating the simultaneous fits to the  $\pi\pi$  and  $K\pi$  mass spectra in different  $x$  intervals. Table I gives the scaling cross sections  $[(s/\beta)d\sigma/dz]$  for  $f^0$ ,  $K^*(1430)$ , and  $S$ , where  $z$  is the fractional energy ( $E/E_{\text{beam}}$ ). The acceptances, which were calculated by Monte Carlo techniques using the full detector simulation, were typically  $\sim 50\%$ . The correction for the decay angle ( $\theta^*$ ) cut was made by our assuming isotropic decay in the c.m. frame,<sup>18</sup> and the established branching ratios<sup>19</sup> were used to include contributions from other decay channels. The error bars in Table I and in Fig. 2 are dominated by the systematic uncertainties coming from the fitting of the mass spectra.

We have compared our results on the tensor mesons with the predictions of the Webber cluster model.<sup>5</sup> In this approach the production rates are determined by the phase space available to the cluster decay, and so the tensor mesons should be suppressed relative to the lighter mesons. The scaling cross sections for  $f^0$  and  $K^*(1430)$  predicted by the Webber Monte Carlo simulation are shown in Fig. 2 together with our data points: The agreement is good. As a result of the large numbers of low-momentum particles which produce overwhelming background for  $x < 0.1$ , our results have been extrapolated to the low- $x$  region by use of the shape predicted by the Webber Monte Carlo simulation. We obtain total multiplicities of  $0.14 \pm 0.04$   $f^0$  and  $0.12 \pm 0.06$   $K^*(1430)$  per hadronic

TABLE I. Differential cross sections  $(s/\beta)d\sigma/dz$  ( $z = E/E_{\text{beam}}$ ) for  $f^0$ ,  $S$ , and  $K^*(1430)$  mesons for different  $x$  values ( $x = p/p_{\text{beam}}$ ).

$x$	$(s/\beta)d\sigma/dz$ (nb GeV <sup>2</sup> )		
	$f^0$	$S$	$K^*(1430)$
0.15	$194 \pm 86$	$98 \pm 30$	$182 \pm 110$
0.25	$80 \pm 35$	$67 \pm 21$	$75 \pm 55$
0.35	$71 \pm 24$	$25 \pm 10$	$61 \pm 45$
0.55	$38 \pm 12$	$6 \pm 4$	$9 \pm 5$

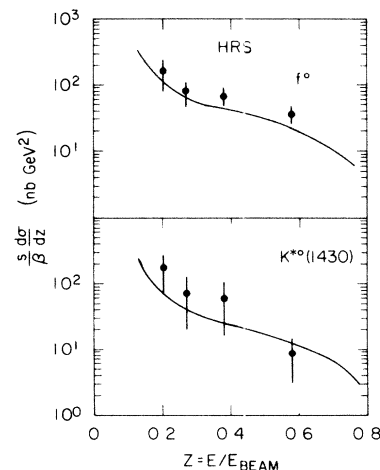


FIG. 2. Scaling cross sections for the production of the  $f^0$  and  $K^*(1430)$  mesons. The solid curves are the predictions of the Webber model.

event, as compared to  $0.95 \pm 0.09 \rho^0$  and  $0.63 \pm 0.10 K^{*0}(892)$  per hadronic event.<sup>20</sup> Without this correction, i.e., for  $x > 0.1$ , the measured multiplicities are  $0.11 \pm 0.04 f^0$ ,  $0.10 \pm 0.06 K^*(1430)$ , and  $0.05 \pm 0.02 S$  per hadronic event. We note that the  $S$ -meson multiplicity is measured to be lower than those of the heavier  $f^0$  and  $K^*(1430)$  mesons.

Since the  $0^{++}$  states are not included in the present version of the Webber Monte Carlo program, the measured  $S(975)$ -meson multiplicity has been compared with the prediction of this model for the production of the  $\eta'(985)$ , assuming a pure  $s\bar{s}$  quark content. The model gives  $0.033 \pm 0.001 \eta'$  per event for  $x > 0.1$ , in good agreement with our measurement of  $0.05 \pm 0.02 S$  per event.

In summary, we observe the production of tensor mesons  $f^0$  and  $K^{*0}(1430)$  and the scalar meson  $S$  in  $e^+e^-$  collisions at PEP. The measured fragmentation functions are compared with those predicted by the Webber cluster model for the production of tensor mesons. These predictions, which are much flatter than the vector-meson fragmentation functions,<sup>1,2</sup> are able to explain our data. The multiplicities of the tensor mesons are 10% to 20% of the vector-meson multiplicities, thus signifying a large suppression. Since the production of the tensor and scalar mesons is not included in the present version of the Lund Monte Carlo program, we have not examined this approach to the production of these states. With the assumption of an  $s\bar{s}$  structure, the Webber Monte Carlo simulation predicts a multiplicity for the  $\eta'$  which agrees well with our measurement of the  $S$ . This may suggest a large strange-quark component in the  $S$  structure, compatible with an  $S$ - $\epsilon$  ideal (or near-ideal) mixing. However, a  $K\bar{K}$  bound state, because of its coupling to an  $s\bar{s}$  system, cannot be ruled out. At present, other four-quark systems and/or gluonic states proposed for the  $S$ -meson structure cannot be examined by these data, since no prediction on their production rates is available.

This work was supported in part by the U.S. Department of Energy under Contracts No. W-31-109-ENG-38, No. DE-AC02-76ER01112, No. DE-AC03-76SF000998, No. DE-AC02-76ER01428, and No. DE-AC02-84ER40125. This experiment was made possible by the support provided by the PEP staff and the technical staffs of the collaborating institutions.

(a)Present address: Lockheed Missiles and Space Co., Sunnyvale, CA 94086.

(b)Present address: Stanford Linear Accelerator Center, Stanford, CA 94305.

(c)Present address: Bell Laboratories, Naperville, IL 60566.

(d)Present address: SRI International, Menlo Park, CA 94025.

(e)Present address: Brandeis University, Waltham, MA 02254.

(f)Present address: CERN, CH-1211 Geneva 23, Switzerland.

<sup>1</sup>M. Derrick *et al.*, Phys. Lett. **158B**, 519 (1985).

<sup>2</sup>W. Bartel *et al.*, Phys. Lett. **145B**, 441 (1984); H. Aihara *et al.*, Phys. Rev. Lett. **53**, 2378 (1984).

<sup>3</sup>B. Anderson *et al.*, Phys. Rep. **97**, 32 (1983).

<sup>4</sup>B. Anderson and S. Gustafson, Lund University Report No. LU TP 82-5 (to be published).

<sup>5</sup>B. R. Webber, Nucl. Phys. **B238**, 492 (1984).

<sup>6</sup>Production of tensor and scalar mesons is observed in  $\psi$  decay. There is also evidence for these productions around the  $Y(1S)$  mass region. See G. Gidal *et al.*, Phys. Lett. **107B**, 153 (1981); S. Behrends *et al.*, Phys. Rev. D **31**, 2161 (1985).

<sup>7</sup>R. L. Jaffe, Phys. Rev. D **15**, 267 (1977).

<sup>8</sup>R. L. Jaffe and K. Johanson, Phys. Lett. **60B**, 201 (1975); D. Robson, Nucl. Phys. **B130**, 328 (1977).

<sup>9</sup>J. Weinstein and N. Isgur, Phys. Rev. Lett. **48**, 659 (1982), and Phys. Rev. D **27**, 588 (1983).

<sup>10</sup>D. Bender *et al.*, Phys. Rev. D **30**, 515 (1984).

<sup>11</sup>We used the function  $\alpha_0(m - m_0)^{\alpha_1} \exp(\alpha_2 m + \alpha_3 m^2)$ , where the  $\alpha_n$ 's are free parameters and  $m_0$  is the appropriate  $\pi\pi$  or  $K\pi$  mass threshold. This function has commonly been used to fit a smooth phase-space background near a mass threshold.

<sup>12</sup>The subtracted spectra contain  $\sim 65\%$  of the original neutral spectra.

<sup>13</sup>The  $K\pi$  mass spectrum contains reflections from  $K^* \rightarrow K\pi$  with the kaon mass assigned to pions and vice versa.

<sup>14</sup>This is the reflection from  $\omega \rightarrow \pi^+\pi^-\pi^0$  decay with one of the charged pions misassigned as a kaon. Reflection of the  $\omega$  decay into the  $\pi\pi$  spectrum is not considered because its effect in the fitted mass region is negligible.

<sup>15</sup>T. Sjostrand, Comput. Phys. Commun. **27**, 243 (1982). Since the present version of the Lund Monte Carlo program does not include the tensor and scalar mesons, we have approximated the  $f^0$  and  $S$  spectra by generating  $\rho$ -meson events with mass and width changed to the values appropriate to the  $f^0$  and  $S$  mesons. Similarly, the  $K^*(1430)$  events were generated by changing of the mass and width of  $K^*(892)$ .

<sup>16</sup>We used the function  $\beta_0 \exp(\beta_1 m + \beta_2 m^2) [1 + \beta_3 |m - \beta_4|^{\beta_5}]^{-1}$ , in which the  $\beta_n$ 's are free parameters.

<sup>17</sup>C. G. Wohl *et al.* (Particle Data Group), Rev. Mod. Phys. **56**, S1 (1984).

<sup>18</sup>This is true if the produced particles are unpolarized, as is the case in the Webber cluster model.

<sup>19</sup>From Ref. 17, the following branching ratios were extracted for the charged decays:  $B(S \rightarrow \pi^+\pi^-) = 52\%$ ,  $B(f^0 \rightarrow \pi^+\pi^-) = 56\%$ , and  $B(K^{*0}(1430) \rightarrow K^\pm\pi^\mp) = 30\%$ .

<sup>20</sup>The Webber Monte Carlo prediction of the vector mesons agrees well with our measurements.